Supporting Information

Compact Hybrid (Gold Nanodendrite-Quantum Dots) Assembly: Plasmon Enhanced Fluorescence-Based Platform for Small Molecule Sensing in Solution

Huide Chen and Yunsheng Xia*

Key Laboratory of Functional Molecular Solids, Ministry of Education; College of Chemistry and Materials Science, Anhui Normal University, Wuhu, 241000, China.

xiayuns@mail.ahnu.edu.cn

1. Preparation of Positively-Charged Gold Nanospheres (AuNSs). Cysteamine modified AuNSs were prepared according to the published method.[1] Briefly, a cysteamine solution (400 μL, 213 mM) was added to 40 mL of 1.42 mM chloroauric acid ($HAuCl_4$) solution. After stirring for 15 min at room temperature, 10 μL of 10 mM freshly prepared sodium borohydride ($NaBH_4$) solution was added, and the mixture was vigorously stirred for 10 min at room temperature in the dark. Then, the mixture was further stirred 20 min, and the resulting win-red solution was stored in the refrigerator (4 °C) and ready for use. The concentration of the AuNSs was estimated by the method reported previously.[2]

2. Finite-Difference Time-Domain (FDTD) Calculations. The FDTD method is an algorithm to solve Maxwell's curl equations on a discretized spatial grid. It can be used to study both surface- and near-field electromagnetic responses of metal nanoparticles with arbitrary shapes. In our simulations, the FDTD calculations were performed using a soft package EastFDTD Solutions

v4.0, developed by Dongjun Technology Co. In all of the calculations, the Au dielectric function was represented as the Drude model,[3] with parameters chosen to match the bulk gold dielectric data.[4] The model of Au nanosphere/dendrite was achieved by 3D Studio Max soft package, the AuNS is modeled as a sphere and AuND is modeled as a sphere plus with tens of cylinders capped with a half sphere at the end. The dimensions were set to be the average experimental values. The surrounding medium for both AuNS and AuND is air, and the refractive index was taken to be 1.0 for the calculations. In addition, a plane wave was used as the excitation source to simulate the interaction with the nanostructure.

3. Supplementary Data

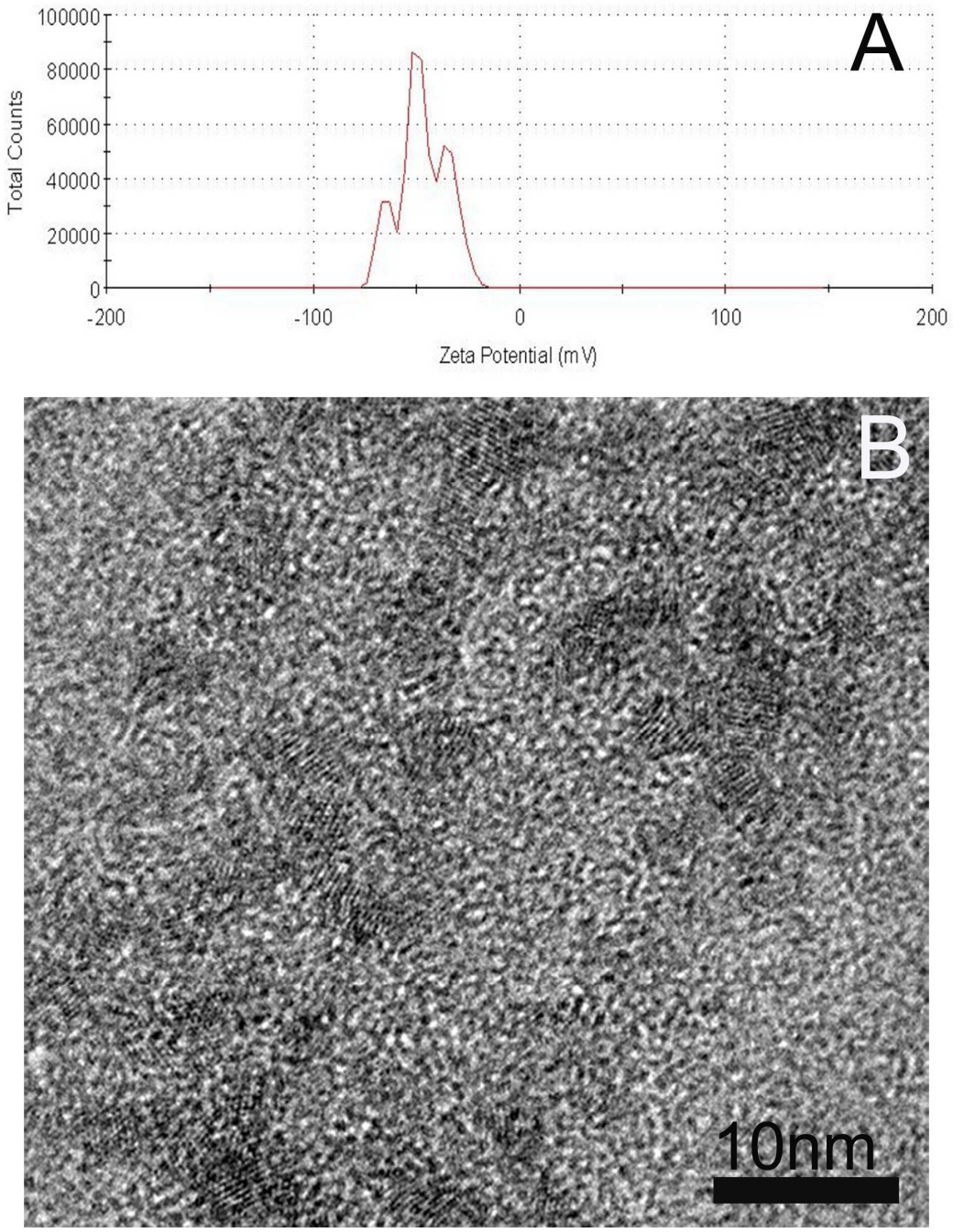

Figure S1. ξ-potential value (A) and TEM image (B) of the TGA-capped CdTe-600 QDs.

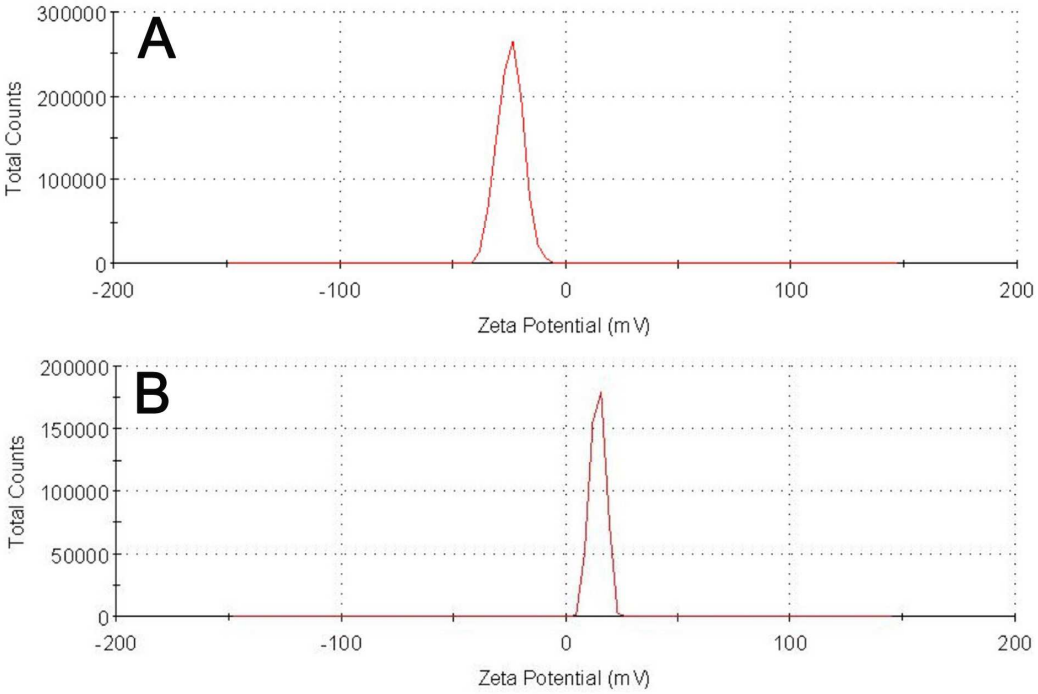

Figure S2. ξ-potential values of unmodified AuNDs (A), cysteamine modified AuNDs (B). To avoid the influence of pH, both of the measurements are controlled at the same pH (6.0). After modification, the ξ-potential values of the AuNDs change from –24.3 to +11.0 mV. These data demonstrate that the cysteamine molecules are successfully bound to the AuND surface.

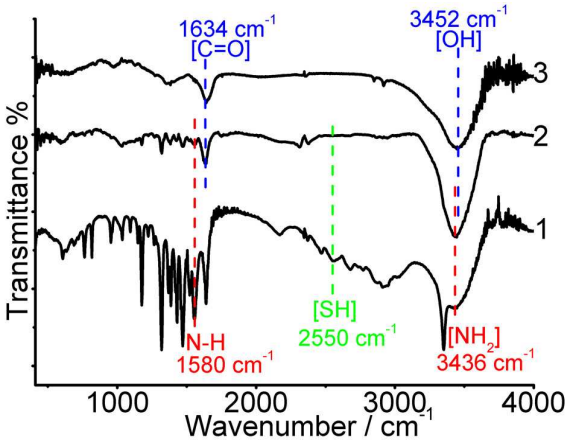

Figure S3. FT-IR spectra of cysteamine (curve 1), cysteamine-modified AuNDs (curve 2), unmodified AuNDs (curve 3). In curve 3, the peak of 3452 cm^{-1} is corresponding to the stretching vibration of hydroxyl group, two peaks at 1634 cm^{-1} and around at 1400 cm^{-1} are associated with the asymmetric and symmetric stretching vibrations of the carboxylic group (COO^-), respectively.[5] The presence of hydroxyl and carboxylic groups in the unmodified AuNDs is because of that citric acid has been used for AuND synthesis. In contrast to curve 3, the absorption band of curve 2 at 3100-3600 cm^{-1} is narrower, and the peak exhibits an observable shift to lower wave numbers (3452 cm^{-1} vs. 3436 cm^{-1}). It is known that both hydroxyl group and amino groups have FT-IR signals at 3100-3600 cm^{-1}. However, the absorption band of amino groups is both narrower and located at lower wave numbers than that of hydroxyl group groups.[5b,6] Then, the peak of 1580 cm^{-1} in curve 2 comes from N-H deformation vibration. Third, the serial peaks from 1300-1500 cm^{-1} in curve 1 are corresponding to deformation vibration of C-H, which can also be found in curve 2. These results clearly indicate that cysteamine molecules are successfully modified on the surface of AuNDs. Furthermore, the absorption of S-H stretching vibration at 2500-2600 cm^{-1} disappears in the modified AuNDs, which indicates that cysteamine molecules are covalently bound to the AuND surface by Au-S bond.[5a,5c]

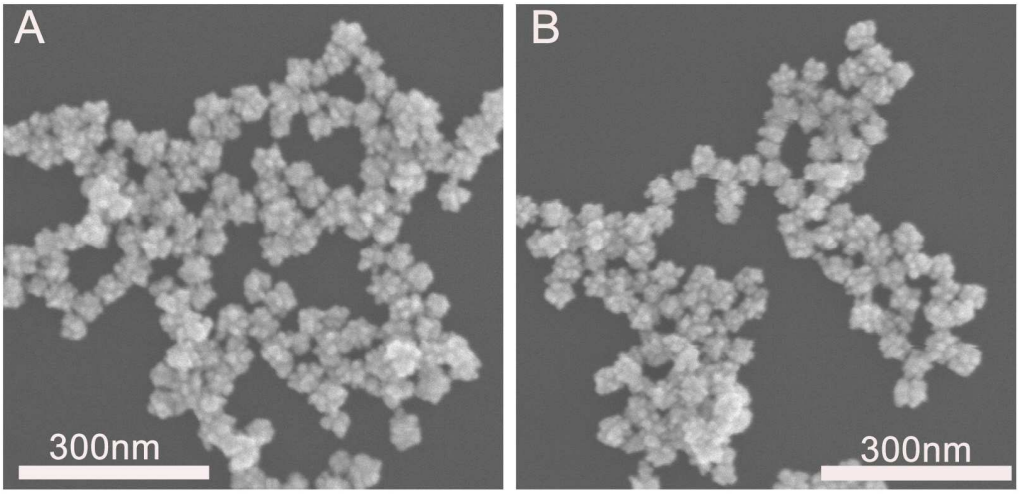

Figure S4. SEM images of AuNDs before (A) and after (B) modification of cysteamine.

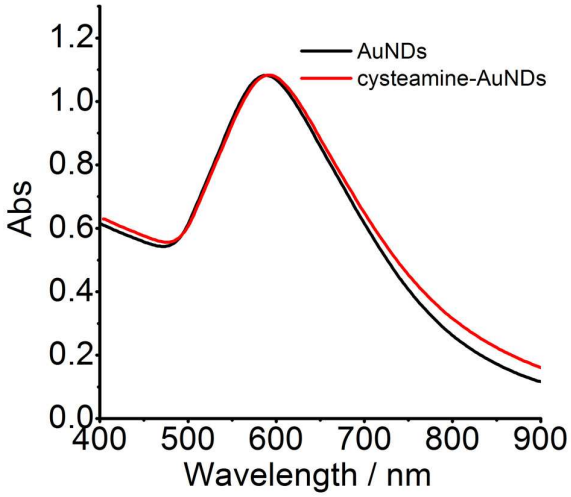

Figure S5. UV-vis absorption spectra of unmodified AuNDs and cysteamine-modified AuNDs.

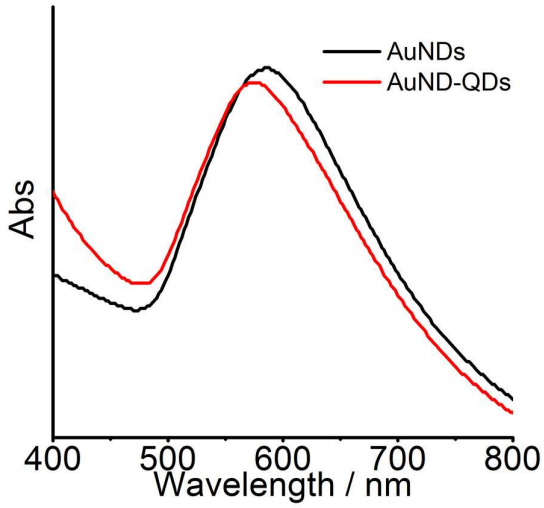

Figure S6. UV-vis absorption spectra of the AuNDs and the (AuND-QDs) assemblies.

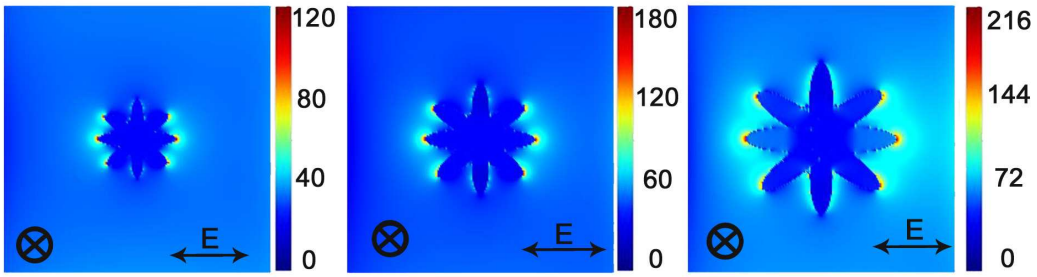

Figure S7. Near-field images of single AuND with three different sizes. The sizes of the three particles are 40 nm (left), 60 nm (middle), 80 nm (right), respectively. Herein, the only difference of the three AuNDs is their size, namely, they possess identical morphology, including subunits, tips and edges, etc. The FDTD calculations indicate: the larger of the AuNDs, the stronger of the electric field. These results demonstrate that larger AuNDs may facilitate to fluorescence enhancement. On the other hand, larger sized particles have stronger scattering effect, which would better quench the enhanced fluorescence emitted from nearby (AuND-QDs) assemblies in bulk solution. Considering the balance of the two effects, there probably has the most appropriate size for solution-PEF. Obviously, the size related PEF behavior is an interesting physicochemical issue deserving further study.

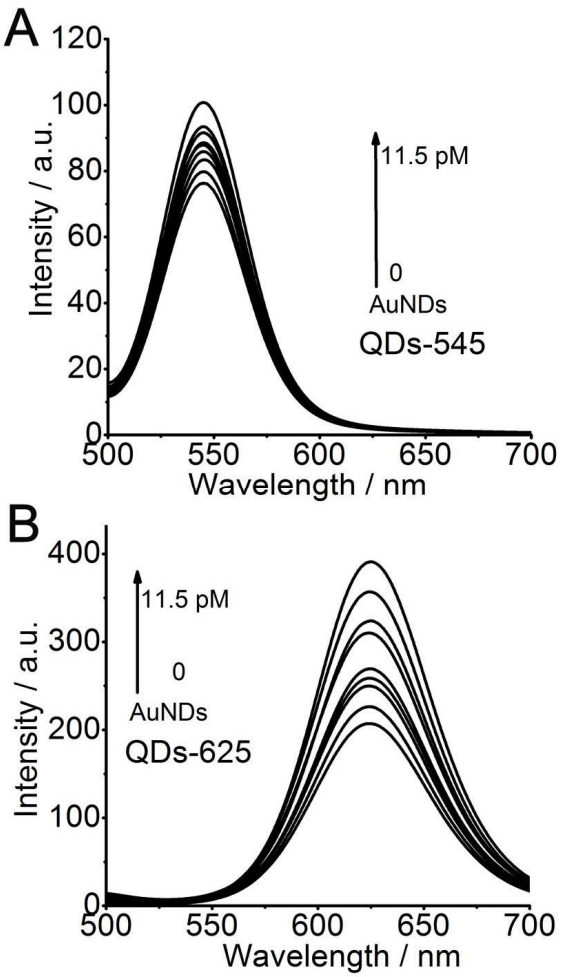

Figure S8. Evolutions of fluorescence spectra of QDs-545 (A), QDs-625 (B) with increasing the AuNDs concentrations.

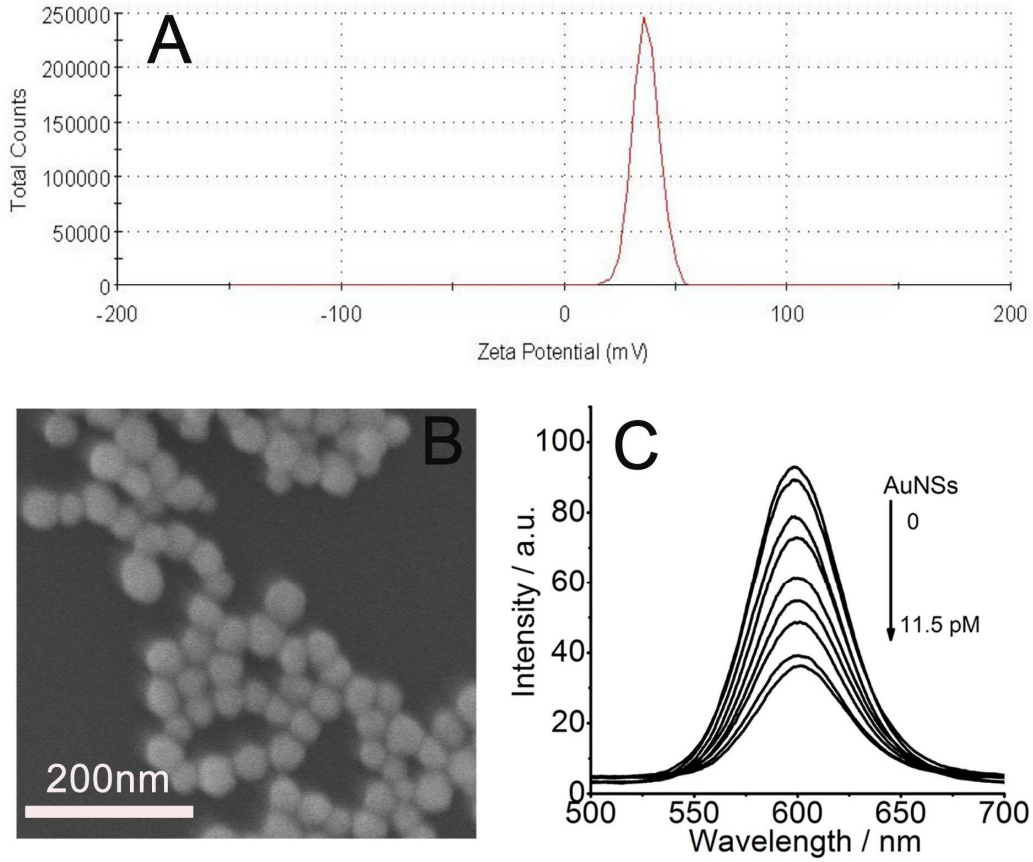

Figure S9. (A) ξ-potential values of gold nanospheres (AuNSs), (B) SEM image of gold nanospheres (AuNSs), (C) evolutions of fluorescence spectra of CdTe@CdS QDs with increasing AuNSs concentrations, the concentration of QDs is 5.7 nM.

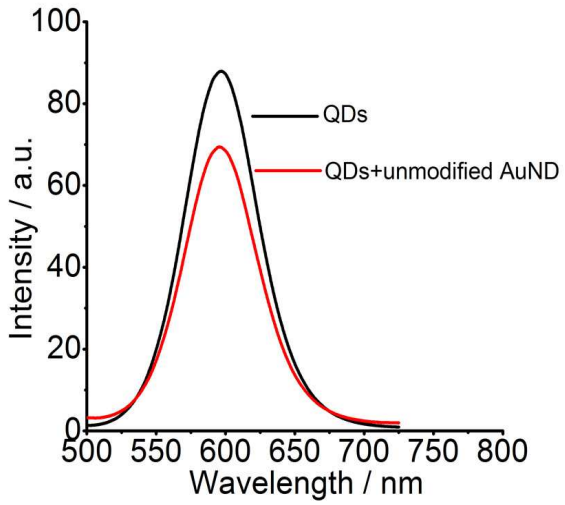

Figure S10. Fluorescence spectra of CdTe@CdS core@shell QDs in the absence and presence of unmodified AuNDs. The concentrations of the QDs and AuNDs are 5.7 nM and 11.5 pM, respectively. In the presence of the AuNDs, the QD fluorescence decreased about 20%, at the same time, the fluorescence profiles kept rather well. These results indicate that the quenching effect probably results from inner filter effect instead of light scattering. On the other hand, this quenching effect is a fixed value for a specific (AuND-QDs) system, which correspondingly does not impact the sensing applications.

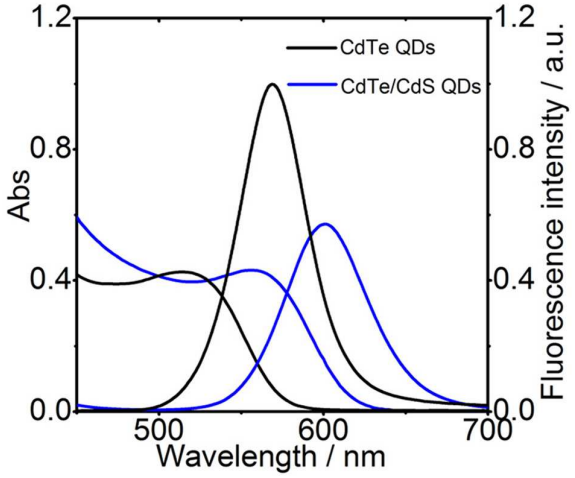

Figure S11. Absorption and fluorescence spectra of CdTe and CdTe@CdS QDs,

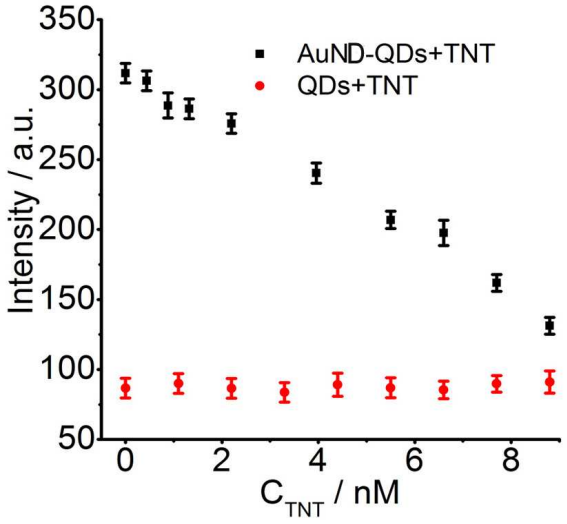

Figure S12. Fluorescence intensity of CdTe@CdS QDs and (AuND-QDs) assemblies in the presence of TNT. The concentrations of AuNDs and QDs are 11.5 pM and 5.7 nM, respectively.

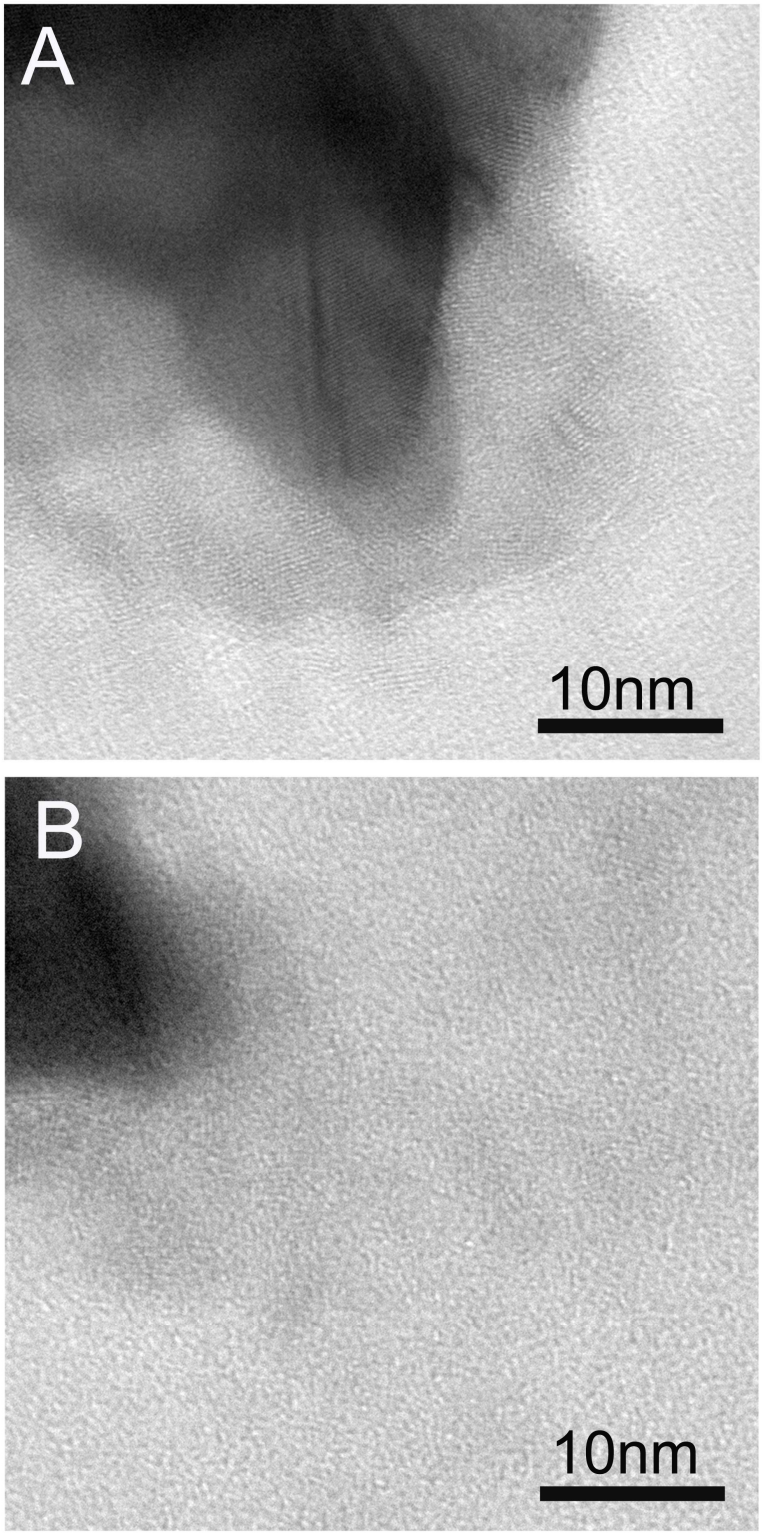

Figure S13. (A) TEM images of the hybrid (AuND-QDs) assembly. (B) TEM images of the hybrid (AuND-QDs) assembly after addition of 8.8 nM TNT. The concentrations of AuNDs and QDs are 11.5 pM and 5.7 nM, respectively.

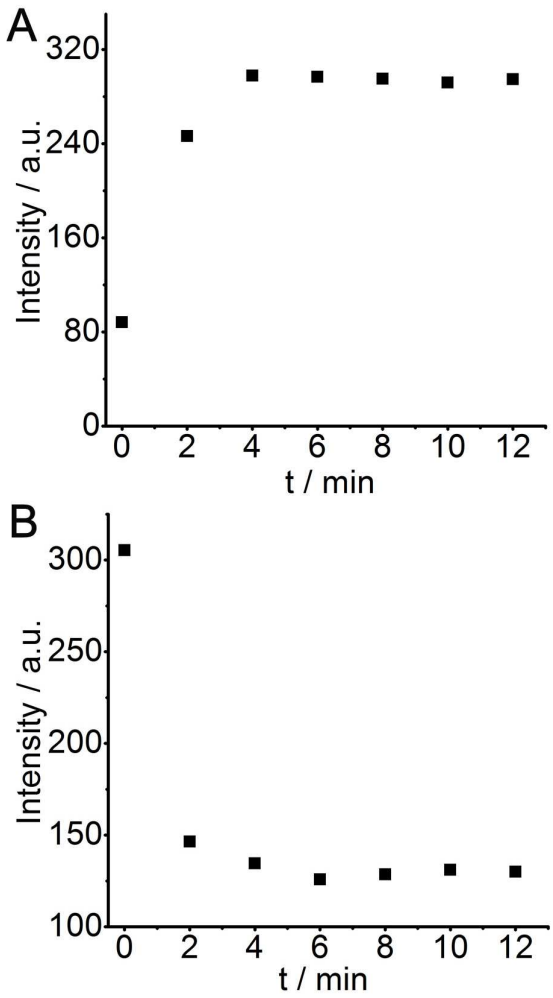

Figure S14. (A) Fluorescence intensity of the CdTe@CdS QDs (5.7 nM) in the presence of 11.5 pM AuNDs as a function of time. (B) Fluorescence intensity of the (AuND-QDs) assemblies with increasing 8.8 nM TNT as a function of time. The concentrations of the AuNDs and the QDs are 11.5 pM and 5.7 nM, respectively.

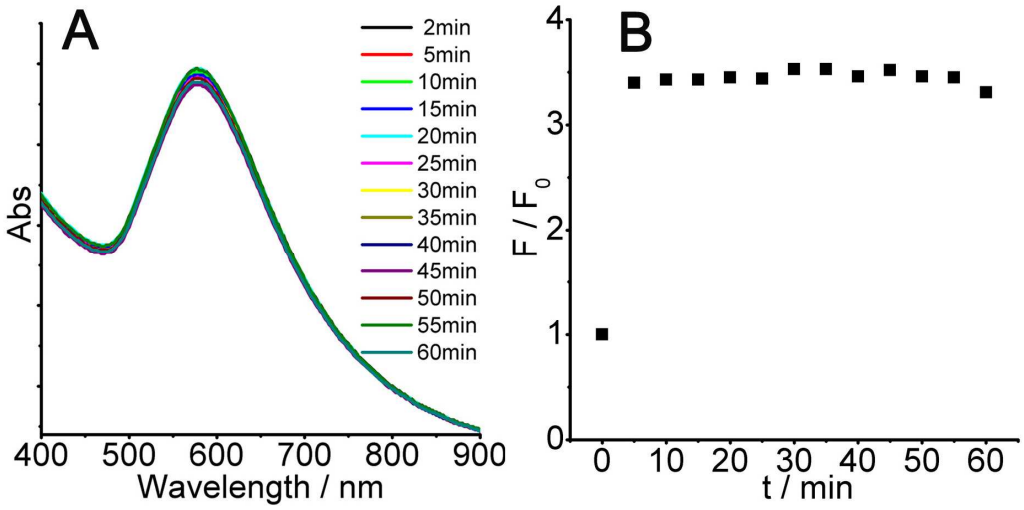

Figure S15. Stability of the hybrid (AuND-QDs) assembly. Absorption spectra (A) and Plots of F/F_0 (B) of the (AuND- QDs) hybrid assemblies. The concentrations of AuNDs and QDs are 11.5 pM and 5.7 nM, respectively.

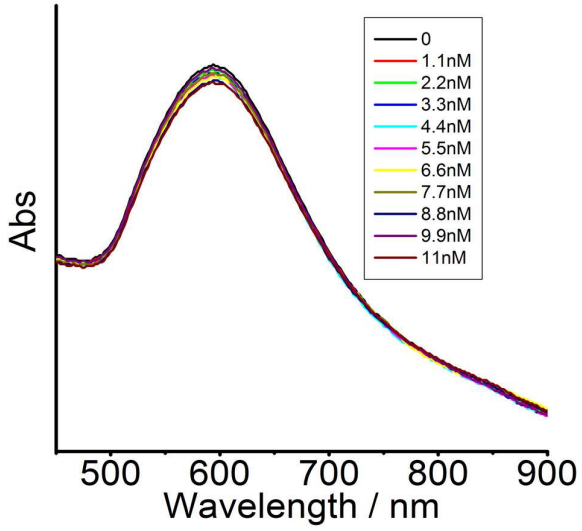

Figure S16. UV-vis absorption spectra of cysteamine-modified AuNDs (11.5 pM) in the presence of vary concentrations of TNT. Based on the absorption spectra, the cysteamine-modified AuNDs did not aggregate in the presence of TNT molecules.

Table S1. Comparison of analytical parameters between the present method and some other fluorescent nanosystems for TNT sensing.

Probes	Linear range (nM)	Limit of detection (nM)	Selectivity[a]	Response mode	Refs.
Mn dopped ZnS QDs	2.5-450	0.8	moderate	quench	7
Au@SiO_2@Ag_{15} meso-flowers	-	0.44	excellent	quench	8
MIP-capped CdTe QDs	800-30000	280	excellent	quench	9
Gold nanorod-QDs	1.1-66	0.1	excellent	turn-on	10
Dye-modified Silica Nanoparticle	10^4-10^5	1	moderate	quench	11
Amine-capped ZnS-Mn^{2+} Nanocrystal	10^4-10^5	1	moderate	quench	12
L-cysteine capped CdTe QDs	-	1.1	excellent	quench	13
CdSe/ZnS QDs	-	0.1	moderate	quench	14
AuND-QDs assembly	0.44-8.8	0.05	excellent	quenching-free	Present work

a. For selectivity, moderate : cannot distinguish TNT from its analogues, such as nitrobenzene and 2,4-dinitrotoluene; excellent: can distinguish TNT from its analogues.

REFERENCES

(1) Jv, Y.; Li, B.; Cao, R. *Chem. Commun*. **2010**, *46*, 8017−8019.

(2) Liu, X.; Atwater, M.; Wang, J.; Huo, Q. *Colloids Surf. B* **2007**, *58*, 3−7.

(3) Oubre, C.; Nordlander, P. *J. Phys. Chem. B* **2004**, *108*, 17740−17747.

(4) Johnson, P. B.; Christy, R. W. *Phys. Rev. B* **1972**, *6*, 4370−4379.

(5) (a) Liu, X.; Jiang, H.; Lei, J.; Ju, H. *Anal. Chem.* **2007**, *79*, 8055−8060. (b) Wang, M.; Mi, C. C.; Wang, W. X.; Liu, C. H.; Wu, Y. F.; Xu, Z. R.; Mao, C. B.; Xu, S. K. *ACS Nano* **2009**, *3*, 1580−1586. (c) Koneswaran, M.; Narayanaswamy, R. *Sens. Actuators B* **2009**, *139*, 104−109.

(6) Kuang, R.; Kuang, X.; Pan, S.; Zheng, X.; Duan, J.; Duan, Y. *Microchim. Acta* **2010**, *169*, 109−115.

(7) Zou, W. S.; Sheng, D.; Ge, X.; Qiao, J. Q.; Lian, H. Z. *Anal. Chem.* **2011**, *83*, 30−37.

(8) Mathew, A.; Sajanlal, P. R.; Pradeep, T. *Angew. Chem. Int. Ed.* **2012**, *51*, 9596−9600.

(9) Xu, S.; Lu, H.; Li, J.; Song, X.; Wang, A.; Chen. L.; Han, S. *Appl. Mater. Interfaces* **2013**, *5*, 8146−8154.

(10) Xia, Y.; Song, L.; Zhu, C. *Anal. Chem*. **2011**, *83*, 1401−1407.

(11) Gao, D.; Wang, Z.; Liu, B.; Ni, L.; Wu, M.; Zhang, Z. *Anal. Chem.* **2008**, *80*, 8545−8553.

(12) Tu, R.; Liu, B.; Wang, Z.; Gao, D.; Wang, F.; Fang, Q.; Zhang, Z. *Anal. Chem.* **2008**, *80*, 3458−3465.

(13) Chen, Y.; Chen, Z.; He, Y.; Lin, H.; Sheng, P.; Liu, C.; Luo, S.; Cai, Q. *Nanotechnology* **2010**, *21*, 125502−125506.

(14) Freeman, R.; Finder, T.; Bahshi, L.; Gill, R.; Willner, I. *Adv. Mater.* **2012**, *24*, 6416−6421.